Biomechanics of the peafowl's crest: a potential mechanosensory role for feathers during social displays

Suzanne Amador Kane*[1], Daniel Van Beveren[1], Roslyn Dakin[2,3]

[1] Physics Department, Haverford College, Haverford, PA 19041, USA

[2] Department of Zoology, University of British Columbia, Vancouver, BC V6T1Z4, Canada

[3] Migratory Bird Center, Smithsonian Conservation Biology Institute, P.O. Box 37012, Washington, DC 20013, USA

*corresponding author: samador@haverford.edu

Running title: Biomechanics of peafowl feather crests

Keywords: feather; mechanoreception; resonance; near-field sensing; peacock; multi-modal signaling

Summary statement: Peafowl crest feathers have mechanical properties that make them suitable for sensing potential airborne signals generated during multimodal social displays.

ABSTRACT

Feathers act as vibrotactile sensors that can detect mechanical stimuli during avian flight and tactile navigation, suggesting that they may also detect signals during social displays. We explored this potential novel sensory modality by studying the biomechanical properties of feather crests that are found on the heads of Indian peafowl (*Pavo cristatus*). We show that these crest feathers are coupled to filoplumes, small feathers known to function as mechanosensors. We also determined whether the airborne stimuli generated by peafowl courtship and social displays couple efficiently via resonance to the vibrational response of feather crests. Vibrational measurements showed that peafowl crests have fundamental resonant frequencies that could be driven near-optimally by the shaking frequencies used by peacocks performing train-rattling displays. Crests were also driven to vibrate near resonance when we played back mechanical sounds generated by these displays in the acoustic very near-field, where such displays are experienced *in vivo*. When peacock wing-shaking courtship behaviour was simulated in the laboratory, the resulting pulsatile airflow excited measurable vibrations of crest feathers. These results suggest that peafowl crests have properties that make them suitable mechanosensors for airborne stimuli generated during social displays. Such stimuli could complement acoustic and visual perception, thereby enhancing the detection and interpretation of social displays. Diverse feather crests are found in many bird species that perform similar displays, suggesting that this proposed sensory modality may be widespread. We suggest behavioral studies to explore these ideas and their functional implications.

INTRODUCTION

A large body of research in mammals and arthropods has found that whiskers, antennae, and hairs play important sensory roles directly related to their vibrational response and mechanical structures (Barth et al., 2012; Sofroniew and Svoboda, 2015). The similar morphology of elongated head feathers in birds raises the question of whether feathers might serve a similar somatosensory function. While most research has focused on their possible role as sexually- or socially-selected traits (Burley and Symanski, 1998; Jones and Montgomerie, 1992; Hagelin, 2002), behavioral studies have shown that head feathers can also function as mechanosensors. Feathers in general are often coupled to vibration-sensitive nerve endings that can allow birds to sense and respond to a variety of mechanical stimuli (Saxod, 1978; Necker, 1985b; Brown and Fedde, 1993). For example, birds change their posture in response to air flows directed at their heads (Bilo and Bilo, 1983), crest feathers can play a mechanosensory role in tactile navigation (Seneviratne and Jones, 2008; Seneviratne and Jones, 2010), and flight, contour, and facial bristle feathers can act as lightweight sensors that provide important information during flight (Bilo and Bilo, 1978; Brown and Fedde, 1993; Brücker et al., 2016) and prey capture (Cunningham et al., 2011). Feather crests and whisker-like plumes are found on the heads of a wide variety of bird species as well as feathered dinosaurs and early fossil birds (Lindow and Dyke, 2006; Li et al., 2010). Because isolated feathers can play a sensory role, feathers may have evolved to serve such functions before they were adapted for thermoregulation and flight (Persons and Currie, 2015).

During social displays, many birds produce sounds, airflow patterns, and substrate vibrations, when they flap or vibrate their wings or tails (Bostwick et al., 2009; Clark et al., 2013a; Ota et al., 2015; Clark, 2016; Dakin et al., 2016). These multimodal displays may stimulate multiple senses, including visual, acoustic and vibrotactile perception. For example, male Indian peafowl ("peacocks", *Pavo cristatus*) attract mates by spreading and erecting the train, a fan-like array of long, colorful feathers, and performing two different shaking behaviors (Fig. 1A, Movie S1). First, in the wing-shaking display, the peacock orients his backside toward nearby females ("peahens") and flaps his partially unfurled wings at approximately 5.4 Hz. Second, in the train-rattling display, the peacock faces a female at close range (approximately 1 to 1.5 m) and shakes his tail and train feathers rapidly at 22-28 Hz (mean = 25.6 Hz), causing his train to shimmer

iridescently and emit a mechanical sound (Dakin and Montgomerie, 2009; Freeman and Hare, 2015; Dakin et al., 2016). Train-rattling performance by peacocks is obligatory for mating success (Dakin and Montgomerie, 2009), and eye-tracking experiments have shown that both wing-shaking and train-rattling displays are effective at attracting and holding the peahen's gaze (Yorzinski et al., 2013). Peahens also perform a tail-rattling display at 25-29 Hz in a variety of contexts (Dakin et al., 2016), suggesting that feather vibrations might serve other communicative functions as well. Peafowl have been reported to respond behaviorally to playbacks of the infrasound (< 20 Hz) component of train-rattling and wing-shaking recordings (Freeman and Hare, 2015).

Sounds, including those generated by animal motions, consist of oscillations of the surrounding medium in both pressure and particle velocity. Animals can detect pressure oscillations using ears and tympanal organs, whereas particle velocity oscillations can be detected using hairs, antennae and feathers (Fletcher, 1992; Larsen and Wahlberg, 2017). Mechanical sounds detectable by vibrotactile sensors are generally experienced in the acoustic near-field, a region close enough to the source that particle velocity can couple to mechanoreceptors via frictional forces (Fletcher, 1992). Near-field communication has been studied in a wide variety of invertebrate terrestrial taxa (Markl, 1983; Greenfield, 2002) and in fish (Sisneros, 2015). For example, in arthropods, many species use filiform hairs to detect near-field particle velocity for predator or prey detection and intraspecies signaling (Greenfield, 2002; Santer and Hebets, 2008; Barth, 2014). However, no research has considered whether birds also use non-auditory senses to detect similar air-borne signals during social displays, or what influence this may have on their social interactions.

One possible means by which peafowl may sense near-field sound is the fan-like crest (Fig. 1A,B), a planar array of feathers oriented in the sagittal plane that is found on the heads of both sexes (Dakin, 2011). Each crest feather has a spatula-shaped iridescent "flag" of pennaceous vanes at the distal end and a long shaft (rachis) that is bare apart from short, sparse barbs along its proximal end (Fig. 1C). Head feathers have been established to play a mechanosensory role in pigeons (*Columba livia*) and some auklet species (Bilo and Bilo, 1983; Seneviratne and Jones, 2008; Seneviratne and Jones, 2010). Vibrotactile auklet crest feathers are reported to be

elongated filoplumes, a type of feather with known mechanosensory function that also features a long, bare shaft with a tuft of short barbs on its distal end (Lucas and Stettenheim, 1972; Brown and Fedde, 1993; Seneviratne and Jones, 2008). Other birds from diverse species spanning several orders are known to have elongated filoplumes on their heads that protrude beyond the contour feathers (Imber, 1971; James, 1986; Clark and de Cruz, 1989; Childress and Bennun, 2002). Filoplumes are found in birds of all orders, including Indian peafowl, and they are located near the bases of all types of feathers, including head, flight, and contour feathers (Lucas and Stettenheim, 1972; Weir and Lunam, 2011). Both contour feathers and filoplumes are associated at their follicles with Herbst corpuscles, a type of vibration-sensitive mechanoreceptor (Necker, 1985a; Necker, 1985b; Brown and Fedde, 1993; Stettenheim, 2000). This suggests that peafowl crest feathers might act as airflow sensors, with a long lever arm that transmits a magnified version of the forces applied to their distal end down to the mechanoreceptor found at their base (Lucas and Stettenheim, 1972).

Moreover, because the peafowl's region of most acute vision is oriented laterally (Hart, 2002), when a peahen gazes at a displaying male, the maximum area of her crest feathers also points toward the peacock's moving feathers (Fig. 1A). This results in an optimal orientation for intercepting airborne vibrations generated by male display behaviors. This geometry, combined with the presence of feathers with known sensory properties along the base of the crest, suggest that it is worth exploring whether the peafowl's crest also may have a somatosensory function during displays.

To consider how to test this hypothesis, we first review the physical acoustics relevant to vibrotactile detection of mechanical sounds. The reader may consult in-depth treatments for more details (Kalmijn, 1988; Blackstock, 2000; Fahy, 2001; Larsen and Wahlberg, 2017). We will consider two types of sound sources: (1) loudspeakers used as laboratory sources of sound that are often modeled as a monopole (i.e., a sphere with oscillating radius); and (2) vibrating body parts (e.g., wings, tails, or trains) that we model as either a dipole (i.e., a sphere with an oscillating position), or as a freely-vibrating circular disk (hereafter, "vibrating disk") because their position oscillates, not their size (Fletcher, 1992; Blackstock, 2000). Each of these models has different predictions for how sound wavelength (λ), source distance (R), source size (A), and

source geometry (e.g., monopole, dipole, etc.) determine the extent of the acoustic far- and near-fields.

The acoustic far-field behavior of a monopole source corresponds to a dominant propagating spherical pressure wave with an amplitude that varies as 1/R, equivalent to a 6 dB decrease in sound pressure level (SPL) when R doubles; its far-field also has a negligible particle velocity term that falls-off as $1/R^2$. While dipoles and vibrating disks have the same far-field pressure wave amplitude 1/R dependence, their sound emission is highly directional and their negligible far-field particle velocity field falls off more rapidly as $1/R^3$ (Fletcher, 1992). As a result, vibrotactile sensors are unlikely to detect acoustic signals in the far-field.

Vibrotactile sensing instead occurs in the flow (reactive) near-field, the region near the sound source where the particle velocity has its greatest magnitude because the air acts as a layer of effectively incompressible fluid that moves with the source (De Bree et al., 2004; Larsen and Wahlberg, 2017). For $R \leq A/6$ (the very near-field), the particle velocity is approximately constant; it falls off with increasing distance and becomes negligible for mechanosensing at approximately $R \approx A$, although there is no definite boundary (Fletcher, 1992; De Bree et al., 2004; Bradbury and Vehrencamp, 2011). For $R > A$, as R increases past the very near-field regime, both the particle velocities and pressure amplitudes continue to decrease until they are of equal magnitude at $2\pi R/\lambda = 1$ for a monopole, and $2\pi R/\lambda = 1.4$ for a dipole (Kalmijn, 1988). However, the criterion relevant for mechanosensation is the enhancement of the absolute magnitude of particle velocity in the very near-field region for which $R \leq A$, rather than the size of the region over which particle velocity is greater than pressure (which for a dipole is $R \leq 0.22 \lambda$) (Rogers and Cox, 1988). The lateral extent of the near-field also depends on source size, A, for an extended (non-point) source. Source surface area also determines the overall magnitude of the particle velocity, which scales as A^2 for a monopole and A^3 for a dipole. Therefore, for larger extended sources (greater A), the very near-field is a larger region with greater particle velocities (Kalmijn, 1988).

The flow near-field is most relevant in bioacoustics when receivers are separated from the sender by a distance no greater than the size of the vibrating source (e.g., wings, trains or tails; $R \leq A$),

and when the sounds are produced with the low frequencies characteristic of locomotion or motions during display behaviors. During the peacock's display, the extent of the flow very-near field agrees with the typical female-male distances, for which $R \leq A = 1.5$ m (a typical peacock train radius) (Dakin and Montgomerie, 2009; Dakin and Montgomerie, 2011).

In this study, we build on these ideas to explore the biomechanics of the peafowl crest and test its potential role as a sensor during peacock displays. We begin by testing the biomechanical properties we would expect these feathers to have to function effectively as tactile sensors of airborne signals. Specifically, they should vibrate efficiently at socially salient frequencies, either to detect shaking by a conspecific individual, or as a form of proprioception to provide feedback to the animal doing the shaking (Kämper and Dambach, 1981; Dambach et al., 1983; Fletcher, 1992). This can be accomplished readily via mechanical resonance, the phenomenon whereby an object responds with maximum amplitude to a driving force that oscillates at one of its natural frequencies of vibration (Fletcher, 1992). Thus, we expect the feather crests to have a vibrational resonant mode that can be excited by the frequencies and motions used during social displays, as is the case for the feather array peacocks use to perform such displays (Dakin et al., 2016). Previous studies of feathers with lengths similar to those found for peafowl crest feathers (Dakin, 2011) have found a wide range of vibrational resonant frequencies much higher than the 26 and 5 Hz used for peacock courtship displays. For example, club-winged manakin (*Machaeropterus deliciosus*) wing feathers similar in length to peafowl crest feathers have a much higher fundamental resonant frequency of 1.5 kHz (Fig. 1 in (Bostwick et al., 2009)), and tail feathers of various hummingbird species with similar lengths have fundamental resonant frequencies that range from approximately 280 Hz to 10 kHz (Fig. 5 in (Clark et al., 2013b)).

To test this hypothesis, we used high-speed video to measure the resonant frequencies of peafowl feather crests and individual crest feathers, and compared them with *in vivo* train- and tail-rattling shaking frequencies (Dakin et al., 2016); similar video-based methods have been used to measure whisker resonance (Hartmann et al., 2003). Because interactions between feathers can influence their resonant frequency and damping (Cummins and Gedeon, 2012), we compared the biomechanics of crests to that of isolated crest feathers. To test whether mechanical sound might cause crest motion in females located in the near-field of train-rattling peacocks, we also

measured deflections of crests that were exposed to audio playbacks in the laboratory of train-rattling and a white noise control.

Next, we considered the peacock's wing-shaking display. We hypothesized that wing-flapping during the wing-shaking display should result in periodic airflow disturbances that could drive significant crest feather motion. To test this hypothesis, we used high-speed video to visualize the responses of peafowl crests to airflow produced by a wing-flapping robot during simulated wing-shaking displays. Because the wing-shaking display is expected to generate pulsatile airflow at a lower frequency (about 5 Hz) as compared to the train-rattling feather vibration frequency (about 26 Hz), the crests are unlikely to vibrate at resonance for both displays. Therefore, we also conducted an experiment to determine how peafowl crests respond to infrequent individual airflow impulses. Together, these experiments provide a first step to evaluating the potential mechanosensory responses of the avian crest during social signalling. We discuss how this can be followed with further behavioral experiments on live animals.

MATERIALS AND METHODS

In vitro samples

All measurements and fitted values are reported as means [95% confidence interval, defined as 1.96 × s.e.m. for normally distributed data], unless noted otherwise. A total of n = 7 male and n = 8 female Indian peafowl (*Pavo cristatus* Linnaeus 1758) head crests with the feathers still mounted in skin were purchased from commercial vendors. A Digital Microscope Pro (Celestron, Torrance, CA USA) was used to examine the base of peafowl crest feathers to determine whether filoplumes were present, using the structural criteria employed in previous studies of this feather type (Imber, 1971; Lucas and Stettenheim, 1972; James, 1986; Clark and de Cruz, 1989; Childress and Bennun, 2002; Williams et al., 2015). Crest length and width measurements were made by hand and from digital photographs of the crest samples and high-resolution scans (0.02 mm/pixel) of single feathers with a ruler included in the sample plane. We used these measurements to compare the morphology of dried crest samples with that of crests on live peafowl in a previous study (Dakin, 2011), including length, width and number of feathers. Because some peafowl, especially females, have non-uniform crest feather lengths

(Dakin, 2011), we also measured the lengths of individual feathers within the dried crest samples to compare with the previous study.

For mechanical testing, we glued the lower side of the crest skin to a ~2.5 cm cube of balsa wood using hot glue (Fig. 1D). An earlier study that compared the resonance of peacock feathers mounted using rigid balsa wood mounts versus a compliant gel found that the compliant mounts resulted in only slightly lower resonant frequencies and reduced amplitudes at frequencies > 50 Hz (Dakin et al., 2016), as expected for a flexible shaft secured by a stiff clamp (Fletcher, 1992). If the crest feathers were closely clustered, the attached skin was first softened in water and the crest was spread to approximate its natural configuration. To study individual, isolated crest feathers, we removed all but three to five feathers (on the outer edges and in the middle) from two male crests and one female crest and analyzed the characteristics of those remaining feathers. Note that because this procedure was necessarily destructive, it precluded any further whole-crest analyses on those samples, so we limited it to only the three crests.

Because earlier research on feather keratin indicated that water content can affect its elastic modulus (Taylor et al., 2004), all samples were stored and all laboratory measurements were performed at 21.1 Cº (range: 20.8-21.5º) and 74.8 % relative humidity (range 72.3-77.7%). For comparison, peacock train-rattling display frequencies were measured in the field at a median temperature of 19.4ºC and a median relative humidity of 60.7% (Dakin et al., 2016), with over half of the displays occurring within ±2.2ºC and ±14% of the average laboratory temperature and relative humidity, respectively. Moreover, a re-analysis of previous published data on 35 peacock displays performed by 12 males in the field (Dakin et al., 2016) shows that there is no significant association between display vibration frequency and relative humidity ($p > 0.45$) when accounting for the date and time of the displays, as well as the identity of the measured individuals.

Vibrational dynamics trials

For vibrational dynamics measurements, the feather assembly was mounted on a model SF-9324 mechanical shaker (Pasco Scientific, Roseville, CA, USA) driven by an Agilent 33120A function generator (Agilent Technologies, Wilmington, DE, USA) (Fig. S1). Two orthogonal directions

of the driving force were used: “out-of-plane”, oriented normal to the plane of the crest; and “in-plane”, oriented parallel to the plane of the crest and in the posterior-anterior axis of the head (Fig. 1D). The first orientation (out-of-plane) corresponds to the geometry when a peafowl either visually fixates the display by orienting one side of the head towards it, or else drives its own crest into vibrations by performing a train- or tail-rattling display (Dakin et al., 2016). The second (in-plane) orientation recreates the geometry when the front of the head is oriented towards the display or when the bird bobs its head during feeding or walking. The vibrational response spectrum was measured using three linear frequency sweeps, shown in Table S1, with rates of frequency increase chosen to be less than the values measured at the start of peafowl displays in an earlier study (Dakin et al., 2016). Each of the 15 crests was tested three separate times in the out-of-plane orientation at the 0-80 Hz frequency range (n = 45 trials). We also ran trials using the following sweep rates to make sure that changing the sweep rate did not reveal new spectral features at very low frequencies or between 80 to 120 Hz: six crests out-of-plane at 0-120 Hz (n = 18 trials), five crests in-plane at the 0-80 Hz range (n = 14 trials), two crests in-plane at 0-120 Hz (n = 2 trials). Finally, we tested three crests out-of-plane after they had been trimmed down to have only three to five isolated crest feathers remaining (3 feathers for male Crest 03, 5 for male Crest 05 and 3 for female Crest 10), at 0-80 Hz (n = 9 trials), to evaluate the vibrational response of isolated crest feathers.

Video analysis

We recorded feather vibrational motions using high-speed video filmed with a GoPro Hero 4 Black Edition camera (720 x 1280 pixels; 240 frames s^{-1}; GoPro, San Mateo, CA, USA). Image and data analysis were performed using custom programs based on the MATLAB 2015a Machine Vision, Signal Processing and Curve Fitting toolboxes (MathWorks, Natick, MA, USA) available on figshare (Dakin et al., 2017). Lens distortion was first removed using the MATLAB Camera Calibration tool. All feather motions analyzed were in the plane of the image, and thus did not require correction for perspective (Biewener and Full, 1992). To analyze feather motion, we first used auto-contrast enhancement and thresholding to track the mean position of the crest feather flags and the shaker mount, and then computed the spectrogram of each object’s tracked position during the frequency sweep using a Hanning filter. This yielded the magnitude, A, of the fast Fourier transform (FFT) at each vibrational drive frequency, f_d, which was divided by the

shaker drive magnitude, A_d, at that frequency to give the drive transfer function (A/A_d). This procedure normalized the data to take into account any frequency-dependent variation in the magnitude of the shaker head response. The Nyquist frequency, which gives the upper bound on measurable frequencies (Smith, 2010), was 120 Hz (half the frame capture rate), and was thus more than four times the typical biological vibration frequencies used during peafowl displays. Finally, the drive transfer function was smoothed over a 1.3 Hz window using a cubic Savitzky-Golay filter and all peaks in the response were fit to a Lorentzian function using nonlinear-least squares fitting to obtain the resonant frequency, f_r, and full-width-half-maximum, Δf, of the spectral power (Smith, 2010). These fits were performed in Origin 8.6 (Originlab, Northhampton, MA, USA). The quality factor, Q (a measure of how sharply defined the resonant frequency is), was computed from $Q = f_r/\Delta f$.

Audio playback experiments and analysis

To determine if peafowl crests can vibrate detectably due to peacock train-rattling, we filmed high-speed video of peahen crest samples placed in the flow near-field of a loudspeaker playing back train-rattling mechanical sounds. To generate audio playback sequences, we used audio field recordings (24-bit, 44.1 kHz, no filtering) of peacock train-rattling displays made using a PMD661 recorder (±1 dB: 20 Hz to 24 kHz; Marantz, New York, NY, USA) and a ME-62 omnidirectional microphone (±2.5 dB: 20 Hz to 20 kHz; Sennheiser, Wedemark, Germany), as described in a previous study (Dakin et al., 2016). Three playback sequences were used (each using sound from a different peacock), with mean rattle repetition rates of 26.7 ± 0.5 Hz; 25.3 ± 0.5 Hz; and 24.6 ± 0.5 Hz. Recordings of train-rattling in the field indicated that rattles are in-phase (i.e., temporally coherent) over bouts approximately 1.2 s in length that are repeated for several minutes during displays (Dakin and Montgomerie, 2009; Dakin et al., 2016). We spliced together bouts with an integer number of rattling periods to form a longer audio playback file with a total duration of approximately 5 min. For the positive control, we played back Gaussian white noise generated using MATLAB's imnoise command (5 min. duration, 24-bit, 44,100 Hz). The FFT power spectrum computed from the white noise sound file had no significant deviation from a flat frequency response from < 1 Hz to 22,000 Hz (FFT computed using a rectangular window to preserve Fourier amplitudes). The root-mean-squared (rms) amplitudes of all

playback recordings and the white noise control were scaled to the same value while also ensuring that no clipping occurred at high amplitude.

Spectrograms from earlier studies of peacock train-rattling indicated that these pulsatile mechanical sounds consist of broadband impulsive rattles with spectral density primarily in the human audible range, emitted at a repetition rate of approximately 26 Hz; they are neither low frequency pure tones, nor are they sound with spectral density predominantly in the low frequency or infrasound regime (Freeman and Hare, 2015; Dakin et al., 2016). Recording and reproducing such pulsatile sounds at a low repetition rate is different from working with pure tones at very low frequencies, because most of the spectral power of these pulsatile sounds is contained at frequencies well above their repetition rate. A useful analogy is that one does not need a specialized speaker to reproduce the sound of bird calls emitted once a second or hand-clapping at 1 Hz with high fidelity, because such sounds are composed primarily of frequencies much higher than 1 Hz. Consequently, in this study, we used equipment rated for frequencies 20 Hz to 20 kHz rather than equipment designed for infrasound. All sound files were played back on a Lenovo Thinkpad T460S computer connected to a 402-VLZ4 mixer (Mackie; preamplifier; < 0.0007% distortion 20 Hz to 50 kHz) and a ROKIT 10-3 G3 10" powered studio monitor (KRK Systems, Fort Lauderdale, Florida, USA; ± 2.5 dB over to 40 Hz to 20kHz, –10 dB at 25 Hz relative to ≥ 40 Hz) with a 25.4 cm diameter subwoofer (A = 12.7 cm). Following (Gerhardt, 1992), we examined re-recordings of the playback stimuli made with the same microphone and recorder used for the original field audio recordings, and found that the resulting waveforms and spectrograms (Fig. S2) had the same temporal features ("rattle" notes) as the original field recordings of train-rattling (e.g., Fig. 4A in (Dakin et al., 2016)).

For playback experiments, the preamplifier volume controls of the mixer were adjusted so that the mean playback SPL was 88 ± 1 dB at 3 m as measured by a Type 2 model R8050 sound level meter (accuracy ±1.4 dB, C-weighting, 30-100 dB, slow 1.0 s setting; Reed Instruments, Wilmington, NC USA). For comparison, previously-reported values for peacock train-rattling mechanical sounds corrected for background noise were given as 67 to 77 dB at R = 3 m (unweighted SPL) (Freeman and Hare, 2015). For our combination of microphone and playback system, the response at 26 Hz was estimated to be reduced by 12.5 dB compared to the audible

range; the increase in playback SPL relative to the reported values accommodates for this attenuation. During playbacks, the background noise with no audio was 58 ± 1 dB SPL. For large speakers, interference between the sound emitted by different parts of the source can produce complex interference patterns of sound direction and intensity for pure tones at regions near the source (Fahy, 2001; Larsen and Wahlberg, 2017). Consequently, we measured SPL at nine different positions across the subwoofer speaker between the center and edges, at distances perpendicular to the speaker between 12.7 cm to 0.5 m. The measured sound amplitudes varied monotonically in both directions, with no measurable variation due to interference.

Female crest samples (n = 3; crests 7, 8, 15) with resonant responses determined in the vibrational dynamics trials were mounted on a tripod at a distance R = A = 12.7 cm away from the subwoofer speaker face to give optimal exposure to the flow near-field (Fig. S2). Vibrational motion of the samples was measured for three separate trials per crest sample per recording using high-speed video (reducing speaker volume to zero and waiting > 5 s in between trials), and the crest motions were tracked and analyzed from video using the methods described above. The duration of train-rattling bouts gave an FFT frequency resolution of ± 0.50 Hz for vibrational response analysis. To minimize direct mechanical coupling via the substrate, the crest samples and speaker were mounted on Sorbothane™ vibration-isolation pads. Because peacocks often display near the edges of thick vegetation, next to natural ground slopes, or next to hard walls (Hillgarth, 1984) (personal observation), anechoic conditions are not required for effective courtship displays or for simulating their mechanical sounds. However, we still chose to minimize reverberations by surrounding the experiment with acoustic tiles and sound absorbing sheets (Audimute, Cleveland, OH USA; audible sound reduction rating: SAA 0.68, NRC 0.65), resulting in an SPL decrease of 5 dB when distance was doubled for $R \geq 0.25$ m. This decrease in SPL is intermediate between the free-field value of 6 dB and a typical reflective room value of 3 dB (Toole, 2008). We also performed negative controls to ensure that reverberations and substrate vibrations did not drive crest vibrations. This was accomplished by inserting a foam tile between the crest samples and the speaker to block particle velocity oscillations and attenuate directional sound pressure waves from the speaker. Thus, any crest vibrations measured during the controls would be due to substrate vibrations, reverberations, transmitted sound pressure waves, and/or other environmental sources.

Simulated wing-shaking experiments

High-speed videos from a previous study were used to determine the frequency and amplitude of wing motions during the peacock's wing-shaking display (Dakin et al., 2016). We used four videos filmed with the wingtip motion closely aligned with the image plane (see Movie S1) that also showed tail feathers with known lengths. The amplitude of wing-shaking motion was defined by the mean diameter of motion circumscribed by the tips of the partly-unfurled wings during this display, which we estimated to be 7.6 cm on average (range 5.5 to 10 cm). To simulate the resulting air motions in the laboratory, we used a robotic mechanism that caused an entire peacock wing to move, such that its plane remained in the same orientation while its distal end circumscribed a circle with the same rotational circulation as found in living birds (Movie S1 and Fig. S3). The peacock wing was mounted on a carbon fiber rod using a balsa wood base that was attached to the wing via adhesive at the shoulder; this rod pivoted about a clevis joint, which allowed the wing axis to move in a vertical circle while the wingspan remained in the vertical plane. At the end opposite the wing, the rod was attached to a circular crank by a universal joint. The crank and attached wing assembly was driven at 4.95 ± 0.05 Hz by a DC motor. While actual wing-shaking involves motions of two wings toward each other, which presumably displaces more air than a single wing, this apparatus used a single flapping wing moving in a slightly larger diameter (14 cm) circle at the wingtips.

To determine how wing-shaking influences the crest of an observing bird, we first determined the location of maximal airflow speed during robotic wing-shaking. Airflow speeds were measured by a model 405i Wireless Hot-wire Anemometer (Testo, Sparta, NJ, USA) oriented with its sensor facing in the same direction as the crest samples; this device has a resolution of 0.01 m/s, accuracy of 0.1 m/s, measurement rate of 1 Hz, and equilibration time of approximately 5 s. To define the airflow pattern around the flapping wing, air speed was sampled at every point on a 5 cm grid, 5-7 times per location. Based on these results, three peahen feather crest samples (Crests 08, 12, and 13) were positioned using a tripod at the vertical midline of the wing located at varying distances from the wing-tips as shown in Fig. S3. The resulting motions of the crests were then filmed using high-speed video as described above in "Video analysis" to quantify the vibrational response of three different peahen crests. To verify

that substrate vibrations did not drive the crest motion, we performed a control by inserting a 3 x 4 ft foamboard in between the crest and wing to block the airflow from the wing motion; this reduced the root-mean-squared crest motion to 14% of its value with wing motion-induced airflow present. For comparison with the wing-shaking frequency during displays, flapping frequencies during ascending and level flight were also measured for 9 peacocks from 6 online videos (Table S2).

Air vortex experiments

To determine the crest's response to impulsive airflow, we used a Zero Blaster vortex gun (Zero Toys, Concord, MA, USA) to generate single air vortex rings of artificial fog (2-4 cm in diameter, 1 cm diameter cross-section, speed 1.8 m/s [95% CI 1.7, 2.0 m/s, range 1.5 - 2.1 m/s]), aimed so as to impact whole crests (n = 2 peacock and 1 peahen) in the out-of-plane orientation. The motion of crest feathers struck by the vortices was measured by tracking the crest position on high-speed video when an intact vortex impacted the crest oriented with its widest cross-section facing the source at 0.5 m from the point of creation. Because we expected such impulses to result in the crest feathers oscillating at their natural frequency, this provided an additional check on our resonant frequency values.

Force measurements

Peacock feather keratin, like other biopolymers, can have a nonlinear elastic response to external stresses (Weiss and Kirchner, 2010). Because the stimuli in the mechanical shaker, audio playback and wing-shaking experiments each exerted different forces and these forces may have had greater magnitudes than those encountered in the field, we wanted to understand how to extrapolate from our laboratory experiments to a lower force regime that is potentially more biologically relevant. Consequently, we measured the elastic mechanical response of peafowl crests to an external bending force applied to the flags of the crest. We studied the static mechanical response of peafowl crests in the single cantilever bending geometry by measuring the relationship between flag displacement and restoring force of the crest in the out-of-plane orientation (Fig. 1D). Force measurements were made using a Model DFS-BTA force sensor (accuracy ± 0.01 N) connected to a LabQuest2 datalogger (Vernier Software & Technology, Beaverton, OR, USA), which was calibrated using known masses. The force sensor was

attached to a thin rectangular plastic blade oriented in the horizontal plane. The edge of the blade was pressed against the midpoint of the flags of the vertically oriented crest to measure the restoring force exerted by the bent crests. The crests were mounted on a micrometer that moved them toward the force sensor and enabled measurement of crest displacement relative to the location at which the crest flag first deformed and the restoring force first became non-zero within measurement error. These measurements were performed for three trials each for three male and three female crest samples. The resulting force vs displacement data were fit to a linear force-displacement model to determine the linearity of elastic bending deformations. This also gave a value of the bending spring constant, k.

Statistical analysis

To analyze sources of variation in whole crest f_r and Q, we fit Gaussian linear mixed effects models with a random effect of crest ID to account for repeated measures of each bird's crest using the nlme 3.1-131 package (Pinheiro et al., 2017) in R 3.3.3 (R Core Team, 2017). We first verified that trial order and frequency sweep rate, two aspects of the experimental design, did not have significant effects on either f_r or Q (all $p > 0.28$). The next step was to evaluate the potential effects of morphological traits that could influence crest resonance. Because our sample size was only 15 crests, we considered models with only one morphological trait predictor, selected from the following list: length, width, number of feathers, percent of unaligned feathers, and percent of short feathers. These morphological traits were fitted as fixed effect predictors. All models also included fixed effects of sex as well as the vibration orientation (either in-plane or out-of-plane). We used AICc to select the best-fit model (Bartoń, 2015) and evaluated significance of the fixed effects in that model using Wald tests. We report $R^2_{\mathrm{LMM(m)}}$ as a measure of the total variance explained by the fixed effects (Nakagawa and Schielzeth, 2013; Bartoń, 2015). We also used the variance components of the best-fit model to calculate the adjusted repeatability, defined as the variance attributed to differences among crests after adjusting for variation explained by the fixed effects (Nakagawa and Schielzeth, 2010). Inspection of the data and model residuals revealed that variance in f_r differed among crests, so when modelling f_r, we specified this heteroscedasticity using the weights argument (Pinheiro et al., 2017).

RESULTS

Morphology

A microscopic examination of peafowl crest feathers reveals that their shafts have associated filoplumes at the base (Fig. 1E) that agree in location and morphology with those shown in micrographs of filoplumes in (Lucas and Stettenheim, 1972; Necker, 1985a).

The average lengths of the whole crest samples used in this study were 5.3 [4.8, 5.7] cm for 8 female crests, and 5.4 [5.1, 5.7] cm for 7 male crests. Fig. 2 shows that this range of crest lengths agrees with that of live peafowl, indicating that the crest samples used in these experiments were fully grown (Dakin, 2011). The average widths of the whole crest samples were 5.5 [4.6, 6.3] cm for the female crests, and 6.1 [5.3, 6.9] cm for the male crests. These width values were approximately 20% (female) to 27% (male) smaller than those found on live birds (Fig. 2). This difference could be due to the crest ornament being spread 1-2 cm more in the sagittal plane by muscle action in the live bird, similar to erectile crest plumage in many other species (Hagelin, 2002), in addition to the effect of skin drying.

All 7 of the male crest samples had feathers of uniform length, defined as ±8% of the mean fully-grown crest feather length. This is also typically observed *in vivo*, where 72% of male *P. cristatus* crests studied in (Dakin, 2011) had feathers of uniform length. In contrast, the majority (6/8, or 75%) of the female crest samples had non-uniform feather lengths (using the same definition above), which was again similar to the previous *in vivo* study, where 77% of females had non-uniform crest feather lengths (Dakin, 2011). On average, the dried female crests had 7.0% [2.1, 11.8] of their feathers shorter than the mean fully-grown crest feather length. Eight out of the 15 crest samples had all feathers oriented in the same plane within ±5º; five of the crests had 7-11% of the feathers unaligned, and two male crests had 22% and 50% unaligned feathers, respectively.

We also studied the morphology of individual crest feathers to understand their unusual structure (Fig. 1C). The average rachis tapered evenly over its 39.90 [38.89, 40.91] mm length and had a mass of 5.1 [4.8, 5.3] mg, and the plume (or flag) added another 2.50 [0.87, 4.06] mg. Unlike

the fully formed barbs in the pennaceous flag, the lower barbs were short (4.1 [3.0, 5.2] mm) and lacked barbules altogether.

Vibrational Dynamics

The vibrational drive transfer functions of peafowl crests had either a single dominant fundamental peak, or in a few cases, a cluster of two to three peaks in a narrowly-defined frequency range, with no evidence that other modes of vibration caused detectable motions of the pennaceous flags. Each main peak agreed well with the expected Lorentzian fit function (mean adjusted-R^2 = 0.97; range [0.91, 0.998]), supporting our choice of shaker amplitudes and frequency sweep rates. (Fig. 3A) The value of $f_r \pm \Delta f/2$ defines the approximate range of drive frequencies over which power is efficiently coupled into the oscillator. Fig. 3B shows that shaking frequencies measured in the field for displaying male and female peafowl (Dakin et al., 2016) lay within $f_r \pm \Delta f/2$ of the crest resonant frequency for both sexes (n = 8 female crests and 7 male crests). When the shaking force was oriented out-of-plane, the mean crest resonant frequency, f_r, was 28.1 [28.0, 28.1] Hz for female and 26.3 [25.9, 26.6] Hz for male crests, respectively. The mean Δf values were 6.2 [4.4,8.0] Hz (females) and 4.3 [4.2, 4.4] Hz (males).

The repeatability of f_r for whole crests was very high at 94%, demonstrating strong and consistent differences among individual crests (Fig. 3B). Analysis of the sources of variation in f_r indicated that 28% of the total variation in f_r could be explained by sex, crest orientation, and the total area of the pennaceous flags (Fig. 3B). The effect of crest orientation was strong and significant, such that out-of-plane vibrations have f_r values approximately 2.4 Hz higher on average ($p < 0.0001$), whereas the sex difference was not significant ($p = 0.87$) and crests with reduced flag area have a slight but non-significant tendency to have higher f_r values ($p = 0.10$). Crest length, width, number of feathers, and the percent of unaligned and short feathers did not explain variation among crests in the value of f_r.

The sharpness of the crest's resonant frequency is indicated by the quality factor, Q (Fig. 3C). The mean Q for peafowl crests vibrated in the out-of-plane orientation (4.8 [4.0, 5.6] for females, 6.2 [5.6, 6.9] for males) was intermediate between that of peafowl eyespot feathers (Q = 3.6-4.5 ± 0.4 and 1.8 ± 0.3, for individual feathers and feather arrays, respectively) and the tail feathers

that drive the shaking, for which Q_1 = 7.8 ± 0.5 (Dakin et al., 2016). This indicates that peafowl crests are moderately-tuned resonators. The quality factor also has implications for undriven vibrations, such as those caused by single gusts of air. These undriven vibrations take place at the crest's natural frequency, $f_o = f_r \text{ sqrt}(1 - ½ Q^{-2})$; this results in an undetectably small shift (≤ 1.2%) relative to measurement errors for our measured Q values of peafowl crests. We discuss the effect of this level of damping on the time behavior of feather vibrations below.

The repeatability of Q was estimated at 47%, indicating moderate differences among crests in Q. Approximately 49% of the variation in crest Q could be explained by sex, crest orientation, and the total area of the pennaceous flags (Fig. 3C). Male crests were significantly more sharply-tuned than those of females ($p < 0.0001$), and crests that had less flag area tended to be more sharply-tuned ($p = 0.03$). Peafowl crests also have more sharply-tuned resonance when they are vibrated out-of-plane ($p < 0.0001$) as compared to the in-plane orientation.

The frequency response of individual crest feathers was generally consistent with that of the whole/intact crests, as the resonant frequencies of isolated feathers in the out-of-plane orientation ranged from 19.2 Hz to 32.4 Hz (Fig. 3B). Note that the complete analysis of vibration data is also available at: https://doi.org/10.6084/m9.figshare.5451379.v3.

Audio playback experiments

An example FFT power spectrum for the vibrational response of a peahen crest sample during audio playback is shown in Fig. 4. For train-rattling audio playback experiments in which the peahen crest samples were located in the flow near-field of the speaker, the vibrational power spectra of the samples had a peak well above noise near the playback train-rattling repetition rate (the effective drive frequency). However, when the white noise recording was played back, the spectral power near the drive frequency was < 4.3% of that found during playbacks. The peak frequency of crest vibrations agreed with the playback train-rattling repetition rate to within 95% CI for all measurements but one, for which it lay within 2.5 s.e.m. Measurements of crest vibrations made with an acoustic foam tile between the speaker and sample had < 11 % of the FFT spectral power at the drive frequency compared to measurements made without the foam; this value placed an upper bound on the contribution of background sources (e.g., room

reverberations, substrate vibrations, etc.) that were not associated with particle-velocity oscillations from the playback stimulus.

Wing-shaking experiments

The simulated wing-shaking experiment resulted in an airflow pattern with speeds ≤ 0.3 m/s. We used the measured positions of maximum airflow speed to determine the locations for three female crest samples for vibrational motion studies. Up to a maximum distance of approximately 90 cm (one sample) and 80 cm (two samples) from the mean wingtip position, the FFT power spectra of the crest flag vibrational motion resulted in a peak that agreed with the wing-shaking frequency within 95% CI (Fig. 5).

The average peacock wing-flapping frequency during ascending and level flight was 5.5 [5.0, 6.1] Hz (Table S2). This frequency agrees with the average frequency of 5.4 Hz (range of individual bird means = 4.5-6.8 Hz) found for wing-shaking display frequencies measured in the field (Dakin et al., 2016).

Air vortex experiments

When ring-shaped air vortices impacted the crests, the barbs responded with clearly visible motion on video with the average amplitude of motion at the flags of 9.4 [4.3, 14.4] mm (Fig. 6A). Analysis of the free vibrational displacement of the crests over time revealed an exponentially decaying sinusoidal response with a mean frequency that agreed within $\leq \pm 0.4\ \Delta f$ with the natural frequency predicted from the measured resonant response of each crest (Fig. 6B), providing a confirmation of our methodology for measuring resonant frequency. Thus, vortices cause the feather crest to vibrate at its natural frequency, with a decrease in amplitude of 13% after 0.2 s (the approximate period of peafowl wing-shaking displays).

Mechanical bending properties

All feather crests exhibited a highly linear elastic response in the bending experiments: force and displacement were linearly related for displacements up to 10.1 [9.1, 11.0] mm (adjusted R^2 = 0.983 [0.978, 0.989]. This allowed us to compute the bending spring constant, k, from the fitted slopes (Fig. S4). The mean bending spring constants for the individual crests ranged from

0.0022 to 0.0054 N/mm with a measurement repeatability of 47% due to the force sensor contacting the crest flag at somewhat different positions during different trials.

DISCUSSION

The findings from this study support a possible role of peafowl feather crests for sensing near-field particle velocity oscillations and airflows generated by their social motor displays. Peafowl crest feathers are shaped like many arthropod sensory hairs (Bradbury and Vehrencamp, 2011), with their long stiff shafts and distal flags well suited to couple frictionally to and bend with local air motions and to exert mechanically amplified forces to vibration-sensitive filoplumes and mechanoreceptors at their bases. Morphometrics confirmed that the crests of different individual peafowl are relatively uniform in length and area, as previously found in live birds (Dakin, 2011). This structural uniformity helps explain their well-defined and narrow vibrational resonances (Fig. 3). We performed several different biomechanical experiments to understand whether the vibrational mechanics of peafowl crests were consistent with a sensory role during social displays. The fundamental resonant vibrational frequencies of peafowl crests agreed closely with the frequencies used during male train-rattling and female tail-rattling displays. This finding also indicates that peafowl crests can be driven efficiently by these stimuli. The similarity of both the resonant frequency and *Q* factor of the crest's vibrational response with that of the train feathers producing the mechanical sound suggests that as a mechanosensor, the crest would be well-matched to this source, but not to environmental sources of noise (Fletcher, 1992). We examined the response of crests to audio playbacks of train-rattling sounds, and verified that train-rattling caused the crests to vibrate detectably near-resonance, whereas exposing them to white noise resulted in no measurable vibrations above background noise levels.

Is this value of crest resonant frequency merely what one would expect for a generic feather, or does it require a specific combination of material properties and structure? The resonant frequency of a feather is determined by many factors, including the outer cortex and inner pith densities of the rachis, the elastic moduli of these materials, and other morphological features of the feather (such as length, rachis taper, rachis cross-sectional geometry, and distribution and mass of barbules) (Dakin et al., 2016). The head feathers of different birds vary both in absolute

length as well as length relative to other body dimensions (e.g., cockatoos in the family *Cacatuidae*, Victoria crowned pigeons *Goura victoria*, and hoopoes *Upopa epops*, all have very long crests, whereas the double-crested cormorant *Phalacrocorax auritus* and tufted titmouse *Baeolophus bicolor* have very short crest feathers). Thus, there is no obvious reason why peafowl crest feathers should have their observed lengths and structures. However, even if we assume for the sake of argument that peafowl crest feather lengths are determined by some constraint, feathers with similar length in other species can have resonant frequencies well over an order of magnitude greater than those of peafowl crest feathers (Bostwick et al., 2009; Clark et al., 2013b). Therefore, the close agreement between the frequencies characteristic of the shaking motions of the long peacock train and tail feathers and vibrational resonance of short crest feathers is striking and unexpected. Future work should explore whether feather crests in other species are spectrally tuned such that their mechanical resonances also agree with behaviorally-relevant potential near-field acoustic signals.

Because the lowest frequency resonant modes of peafowl crests are about five times the frequency of peacock wing-shaking displays, it seemed unlikely that wing-shaking would drive resonant vibrations of the crest feathers based on their Q values. Therefore, we were surprised to find that the wing-flapping motions used to simulate this display in the laboratory at a distance of ≤ 80 cm from the crest also resulted in crest deflections of several mm. This implies that the airflow impulses generated by the wing-shaking display can also stimulate the feather crests of nearby females. To understand the crest response at a frequency so far from resonance, we measured the deflection of peafowl crests when they were struck by individual air vortices. We found that the crests vibrated near resonance only briefly and then returned close to equilibrium after a time comparable to the period of peacock wing-shaking displays, consistent with their observed Q values. Thus, the airflow due to wing-shaking constitutes a series of essentially distinct impulses that can drive detectable crest responses when air flow disturbances are of sufficient magnitude. Interestingly, peacocks also tilt their trains fore-and-aft during train-rattling at approximately 1 Hz, although we have not yet tested whether the airflows generated by these slower maneuvers can also influence the crest. These results also suggest a novel design for making sensitive biomimetic detectors for sensing impulsive or periodic airflows. Such devices are required for proposed robotic applications of air vortex rings and other airflow

signals as a communication channel (Russell, 2011). The addition of an extremely lightweight pennaceous flag to a cantilever made from a resistance-based flex sensor would enable the flex sensor to experience a large torque from a small force, with a minimal increase in mass.

Static mechanical tests also showed that the peafowl feather crest flags deflect linearly with bending force. Therefore, if we extrapolate the measured mechanical displacement to the low-amplitude regime that likely holds in actual peafowl displays, this suggests that the magnitude of deflections found when the feather crests were exposed to experimental stimuli in this study are consistent with a potential sensory role. It is important to note that neural processes can result in exquisitely small thresholds for mechanosensation. For example, pigeons can detect submicron threshold vibrational amplitudes applied to flight feathers (Shen, 1983; Hörster, 1990), mammalian hair cells are sensitive to sub-nanometer displacements and 0.01 deg rotations (Crawford and Fettiplace, 1985), tactile receptors in human skin are sensitive to submicron vibrational amplitudes (Löfvenberg and Johansson, 1984), and insect filiform hairs are sensitive to airspeeds as low as 0.03 mm s^{-1} (Shimozawa et al., 2003). Further histological and electrophysiological studies of the receptors at the base of avian crest feathers and their associated filoplumes are needed to determine their sensitivity to the types of stimuli studied here.

The hypothesis that feathers might help detect airborne signals also suggests a new way to conceptualize behavioral experiments on birds that produce similar impulsive sounds at low repetition rates. Because infrasound and low frequency sound are transmitted effectively over large distances, most studies on low frequency mechanical or vocal sound reception in birds have used speakers located several meters from the intended animal receivers. For example, male ruffed grouse (*Bonasa umbellus*) were found to respond behaviorally to playbacks of wing beating "drumming" displays (peak frequency 45 ± 6 Hz) conducted 35-40 m away (O'Neil et al., 2018) and male houbara bustards (*Chlamydotis undulata undulata*) responded behaviorally to distant (175 ± 56 m) playbacks of low frequency (fundamental frequency 40-54 Hz) boom vocalizations (Cornec et al., 2017). In both cases, such mechanical sounds are received at similar distances during actual displays. Capercaillie (*Tetrao urogallus*) males also produce mechanical sound when they perform their "flutter-jump" wing-shaking displays (Lieser et al.,

2005). Experiments designed to study this display found no behavioral response when females were exposed to playbacks of the infrasound (≤ 20 Hz) component of flutter-jump recordings produced by speakers located 5 m away (Lieser et al., 2006). In another study, peafowl were reported to respond behaviorally to playbacks of the infrasound components of train-rattling and wing-shaking displays using rotary subwoofers located 5-20 m away from the birds studied (Freeman and Hare, 2015). These experimental designs were appropriate for the stated purpose of determining the response of birds to infrasound or low frequency sound pressure waves at these large distances. However, these playbacks were not conducted with receivers in the flow near-field (i.e., $R \leq A$), so they were not designed to reproduce particle velocity oscillations or airflows due to nearby displays. On a related note, behavioral studies of very low frequency auditory thresholds in birds have found that that some bird species (chickens *Gallus gallus domesticus*, and pigeons *Columba livia*, but not budgerigars *Melopsittacus undulatus*, or mallard ducks *Anas platyrhynchos*) can detect pure tones in the low frequency and infrasound regimes, but only when their eardrums are not perforated (Heffner et al., 2013; Hill et al., 2014; Heffner et al., 2016; Hill, 2017). However, these tests did not probe the kind of impulsive low repetition rate mechanical sounds considered here, and their speakers also were not located in the flow near-field. One study of budgerigars did measure the auditory response to amplitude-modulated low repetition rate pulses, somewhat similar to the mechanical sounds of interest here (Dooling and Searcy, 1981); this work found that the auditory threshold for such sounds resembled a low-pass filter with an optimal, flat response below approximately 40 Hz. However, the audio methods were not described in sufficient detail to determine whether near- or far-field conditions applied (Dooling and Searcy, 1981).

Given the lack of studies of flow near-field sound reception in birds, it would be of great interest to study birds that produce very low frequency sounds that are received by conspecifics located in this regime. For example, cassowaries (genus *Casuarius*) produce sound with fundamental frequencies of 23 or 32 Hz using vocalizations that make their entire bodies vibrate; nearby humans are reported to both hear and feel these vibrations, suggesting that this display likely produces vibrotactile sensations in nearby conspecifics as well (Mack et al., 2003). In the future, audio playback and auditory threshold experiments in birds could be conducted in the flow near-fields to explore such possibilities. Also, apart from the peafowl data cited above, we only know

of a few other studies that have measured sound levels for displays. Audible bird wing-beat sound levels for much smaller species were reported at 64-66 dB SPL and 54-60 dB SPL at 1 kHz and 25 kHz, respectively, at 1.2 m for Eastern phoebes (*Sayornis phoebe*) and chickadees (*Poecile atricapillus*) (Fournier et al., 2013), and ≤ 67.6 dB SPL at approximately 1.0 m for crested pigeons (*Ocyphaps lophotes*) (Hingee and Magrath, 2009), although no details about SPL measurement methods were given in the previous two studies. Ruffed grouse drumming (a wing-beating display) was reported to correspond to 66.2 dB SPL at 1 m (bandwidth 300 Hz to 8 kHz, frequency weighting not reported) (Garcia et al., 2012). No measurements of particle velocities associated with such displays have been reported so far, although suitable sensors exist for taking these measurements (De Bree, 2003).

Peafowl are not the only bird species that have crests and perform shaking displays; for example, we have compiled a list of at least 35 species distributed over 10 avian orders that have both of these traits (Table S3). Given that feathers are known to function as airflow sensors during flight, it is easy to imagine how they could be co-opted to function as sensors during social signaling. Many external stimuli and animal motions produce incidental sounds and airflows that could stimulate these feathers, which could eventually be adapted for a sensory function. For example, females could use air-borne vibrations associated with peacock wing-shaking displays to determine kinematic parameters, such as wingflap frequency, amplitude, and/or duration, that may serve as signals of flight muscle performance (Clark, 2016). Similarly, females may use airborne stimuli generated by the train-rattling display, in which males move the large train ornament with rapid muscular contractions as an indicator of male muscle power and endurance. Males could also sense air-borne stimuli from their own train-rattling displays as a form of proprioception. Testing these hypotheses requires behavioral experiments.

Our results therefore raise the important question of whether birds respond behaviorally to airborne signals detected by their crests. This can be tested using approaches similar to those used in studies that recently demonstrated that flight sounds function as alarm signals (Coleman, 2008; Hingee and Magrath, 2009; Murray et al., 2017). In peafowl, behavioral experiments could test the function of the female crest in a number of ways. A first step would be to blindfold females and test whether airborne stimuli at the socially salient frequencies elicit a

behavioral response. Further experiments could test the function of the crest during male courtship displays by removing or altering the female crest and then examining how females respond to male displays. One way to do this would be to apply a thin coat of clear varnish to the rachis of the crest feathers; this would stiffen the rachis and increase resonant frequency without affecting the crest's visual appearance (i.e., its size or flag iridescence). Similar manipulations could also be performed on male crests, to test whether males use proprioception from the crest to modulate their own vibration displays. The movement of females during displays could also be examined in relation to the airflow patterns generated by wing-shaking peacocks, to test whether female movements are correlated with specific airflows generated by the males. These correlative results could then be tested experimentally by measuring the behavioral response of peahens to puffs of air directed toward specific regions of their plumage, to see how this influences attention and body orientation.

Thus far, the elaborate shape and size of bird feather crests has led to an emphasis on their visual appearance. Many avian courtship displays also involve wing-shaking, tail-fanning and mechanical sound production that may be detected by nearby females in the vibrotactile channel (Table S3). Given the growing interest in multisensory signaling, it seems worth pursuing behavioral studies to investigate the possibility of vibrotactile stimulation. For example, experiments have shown that that male African crickets (*Phaeophilacris spectrum*) signal to females using air vortices produced by wing flicks that are detected by hair-like cerci (Heinzel and Dambach, 1987; Heidelbach and Dambach, 1997; Lunichkin et al., 2016). Other arthropods use mechanoreception for predator or prey detection, and both insects and arachnids communicate via airborne tactile signals (Markl, 1983; Santer and Hebets, 2008; Steinmann and Casas, 2017). The close match between the biomechanics of peafowl crests and peafowl social displays suggest that it is time to explore whether birds use their feathers for vibrotactile sensing in similar ways.

FIGURE LEGENDS

Fig. 1. Peafowl crest feathers have a morphology suitable for detecting mechanical signals during displays. (A) A peahen (foreground) with the plane of her crest oriented towards the displaying peacock (background) as he performs train-rattling vibrations. (B) Both sexes have a crest with an inverted pendulum shape made up of between 20-31 feathers. This photo shows an adult male measured *in vivo*. (C) A single crest feather showing the pennaceous flag at the distal end. Note that only short, thin barbs are present on the relatively bare rachis (shaft) at the proximal end. (D) A whole crest sample mounted for the laboratory experiments. The two axes of vibrational motions ("in-plane" and "out-of-plane") are indicated. (E) Mechanosensory filoplumes (circled) are located at the base of the peafowl crest feathers.

Fig. 2. Morphology of the whole crest samples as compared to that of live peafowl crests. Crests (n = 8 female, n = 7 male) measured *in vivo* (means shown to the right of each data column) had similar morphology to the dried samples, except that the crests on live birds tended to be wider. Dried sample dimensions were measured to the nearest 0.1 cm. Each crest sample is indicated by a unique symbol-color combination.

Fig. 3. Vibrational resonance properties of peafowl crests and individual crest feathers. (A) Vibrational spectrum and Lorentzian fit for peacock crest sample Crest 01. (B-C) Data on crest resonant frequency, f_r, and quality factor, Q. Each dried crest sample (n = 8 female, n = 7 male) is indicated by a unique symbol-color combination, consistent with Fig. 2. (B) The resonant frequency, f_r, of the crest is a close match for the range of vibrational frequencies used during peafowl social displays. As an indication of measurement error, the average 95% CI for each f_r estimate spans 0.072 Hz. The gray shaded area is the range of vibrational frequencies of the train-rattling display, with dotted lines showing the means for displays performed by peacocks (blue) and peahens (green) (Dakin et al., 2016). Variation in f_r was influenced by the vibrational orientation and was also associated with the sex of the bird and the area of pennaceous flags at the top of the crest (although the association with flag area was not statistically significant). The first panel in (B) also shows how a small sample of single crest feathers (n = 3 from male Crest 03, n = 5 from male Crest 05, and n = 3 from female Crest 10)

had a similar range of resonant frequencies as the whole crests vibrated in the same out-of-plane orientation. (C) The quality factor, *Q*, was also influenced by the vibrational orientation, and was associated with the sex of the bird and the area of pennaceous flags. The average 95% CI for each *Q* estimate spanned 0.233. Black horizontal lines in (B-C) are means.

Fig. 4. Effect of audio playback on crests. Vibrational response of a peahen crest (Crest 08) exposed to audio playback in the near-field of the speaker. The FFT spectral power during playback of train-rattling sound (dotted line, plotted on a linear scale on the y-axis) has a peak near the resonant frequency of the crest. The spectral power values recorded during white noise playback (solid line) and when the train-rattling audio was blocked by a foam tile (red dashed line) are also shown.

Fig. 5. Effects of simulated wing-shaking displays. Vibrational response of a female peahen crest (Crest 13) exposed to airflow from a robot that simulated 5.0 Hz peacock wing-shaking displays at a distance 50 cm from the moving wingtip (see also Fig. S3). Note that the FFT spectral power (y-axis) is plotted on a linear scale.

Fig. 6. Displacement of the crest in response to air vortices. (A) Time series showing the change in flag position after a peacock crest (Crest 09) was impacted by a moving vortex of air. When peafowl crests were impacted by such air ring vortices, they deflected measurably, oscillating at their resonant frequency with an amplitude that decayed to a few percent of the initial value over the period of the peacock's wing-shaking display. (B) Mean resonant frequencies (f_r) and mean vortex response frequencies (± 95% CI) for three crests in the vortex experiment.

Acknowledgments

We are grateful to Maarten Hesseling for assistance with preliminary vibrational measurements, Robert Beyer, Robert Lukasik, and Roger Hill for help with instrumentation design and construction, and Robert Koch, Holger Klinck, and Carr Everbach for advice about reproducing pulsatile sounds. We express our gratitude to two anonymous reviewers and James Hare for helpful comments on an earlier version of the manuscript.

Competing interests

The authors declare no competing or financial interests.

Author contributions

Conceptualization: S.A.K.; Methodology: S.A.K., D.V.; Investigation: S.A.K., D.V.; Data curation: S.A.K., D.V., R.D.; Analysis: S.A.K., R.D., D.V.; Writing – original draft: S.A.K., R.D.; Writing – review & editing: S.A.K., R.D., D.V.

Funding

This work was supported by Haverford College and a National Sciences and Engineering Research Council of Canada (NSERC) Postdoctoral Fellowship to R.D.

Data availability

Data and analysis are available from Figshare at: https://doi.org/10.6084/m9.figshare.5451379.v3

References

Barth, F. G. (2014). The Slightest Whiff of Air: Airflow Sensing in Arthropods. In *Flow Sensing in Air and Water*, pp. 169–196. Berlin: Springer.
Barth, F. G., Humphrey, J. A. C. and Srinivasan, M. V. (2012). *Frontiers in Sensing: From Biology to Engineering*. Berlin: Springer Science & Business Media.
Bartoń, K. (2015). *MuMIn 1.15.6*.
Biewener, A. A. and Full, R. J. (1992). Force platforms and kinematic analysis. In *Biomechanics - Structures and Systems: A Practical Approach* (ed. Biewener, A. A.), p. IRL Press.
Bilo, D. and Bilo, A. (1978). Wind stimuli control vestibular and optokinetic reflexes in the pigeon. *Naturwissenschaften* **65**, 161–162.
Bilo, D. and Bilo, A. (1983). Neck flexion related activity of flight control muscles in the flow-stimulated pigeon. *J. Comp. Physiol.* **153**, 111–122.
Blackstock, D. T. (2000). *Fundamentals of Physical Acoustics*. New Jersey, USA: John Wiley & Sons.
Bostwick, K. S., Elias, D. O., Mason, A. and Montealegre-Z, F. (2009). Resonating feathers produce courtship song. *Proc. R. Soc. Lond. B Biol. Sci.* rspb20091576.
Bradbury, J. W. and Vehrencamp, S. L. (2011). In *Principles of Animal Communication*, p. page 30. Sunderland, USA: Sinauer.
Brown, R. E. and Fedde, M. R. (1993). Airflow sensors in the avian wing. *J. Exp. Biol.* **179**, 13–30.
Brücker, C., Schlegel, D. and Triep, M. (2016). Feather vibration as a stimulus for sensing incipient separation in falcon diving flight. *Nat. Resour.* **7**, 411.
Burley, N. T. and Symanski, R. (1998). “A taste for the beautiful”: Latent aesthetic mate preferences for white crests in two species of Australian grassfinches. *Am. Nat.* **152**, 792–802.
Childress, R. B. and Bennun, L. A. (2002). Sexual character intensity and its relationship to breeding timing, fecundity and mate choice in the great cormorant *Phalacrocorax carbo lucidus*. *J. Avian Biol.* **33**, 23–30.
Clark, C. J. (2016). Locomotion-induced Sounds and Sonations: Mechanisms, Communication Function, and Relationship with Behavior. In *Vertebrate Sound Production and Acoustic Communication*, pp. 83–117. Switzerland: Springer, Cham.
Clark, G. A. and de Cruz, J. B. (1989). Functional interpretation of protruding filoplumes in oscines. *The Condor* **91**, 962–965.
Clark, C. J., Elias, D. O., Girard, M. B. and Prum, R. O. (2013a). Structural resonance and mode of flutter of hummingbird tail feathers. *J. Exp. Biol.* **216**, 3404–3413.
Clark, C. J., Elias, D. O. and Prum, R. O. (2013b). Hummingbird feather sounds are produced by aeroelastic flutter, not vortex-induced vibration. *J. Exp. Biol.* **216**, 3395–3403.
Coleman, S. W. (2008). Mourning dove (*Zenaida macroura*) wing-whistles may contain threat-related information for con- and hetero-specifics. *Naturwissenschaften* **95**, 981.
Cornec, C., Hingrat, Y., Aubin, T. and Rybak, F. (2017). Booming far: the long-range vocal strategy of a lekking bird. *Open Sci.* **4**, 170594.
Crawford, A. C. and Fettiplace, R. (1985). The mechanical properties of ciliary bundles of turtle cochlear hair cells. *J. Physiol.* **364**, 359–379.
Cummins, B. and Gedeon, T. (2012). Assessing the Mechanical Response of Groups of Arthropod Filiform Flow Sensors. In *Frontiers in Sensing*, pp. 239–250. Springer, Vienna.

Cunningham, S. J., Alley, M. R. and Castro, I. (2011). Facial bristle feather histology and morphology in New Zealand birds: Implications for function. *J. Morphol.* **272**, 118–128.
Dakin, R. (2011). The crest of the peafowl: a sexually dimorphic plumage ornament signals condition in both males and females. *J. Avian Biol.* **42**, 405–414.
Dakin, R. and Montgomerie, R. (2009). Peacocks orient their courtship displays towards the sun. *Behav. Ecol. Sociobiol.* **63**, 825–834.
Dakin, R. and Montgomerie, R. (2011). Peahens prefer peacocks displaying more eyespots, but rarely. *Anim. Behav.* **82**, 21–28.
Dakin, R., McCrossan, O., Hare, J. F., Montgomerie, R. and Kane, S. A. (2016). Biomechanics of the peacock's display: How feather structure and resonance influence multimodal signaling. *PLOS ONE* **11**, e0152759.
Dakin, R., van Beveren, D. and Amador Kane, S. (2017). Statistical supplement to: Biomechanics of the peafowl's crest: a potential mechanosensory role for feathers during social displays. https://doi.org/10.6084/m9.figshare.5451379.v3.
Dambach, M., Rausche, H.-G. and Wendler, G. (1983). Proprioceptive feedback influences the calling song of the field cricket. *Naturwissenschaften* **70**, 417–418.
De Bree, H.-E. (2003). The microflown: an acoustic particle velocity sensor. *Acoust. Aust.* **31**, 91–94.
De Bree, H.-E., Svetovoy, V., Raangs, R. and Visser, R. (2004). The very near field: theory, simulations and measurements of sound pressure and particle velocity in the very near field.p. St. Petersburg, Russia.
Dooling, R. J. and Searcy, M. H. (1981). Amplitude modulation thresholds for the parakeet (*Melopsittacus undulatus*). *J. Comp. Physiol.* **143**, 383–388.
Fahy, F. J. (2001). *Foundations of Engineering Acoustics*. London: Academic Press.
Fletcher, N. H. (1992). *Acoustic Systems in Biology*. New York, USA: Oxford University Press.
Fournier, J. P., Dawson, J. W., Mikhail, A. and Yack, J. E. (2013). If a bird flies in the forest, does an insect hear it? *Biol. Lett.* **9**, 20130319.
Freeman, A. R. and Hare, J. F. (2015). Infrasound in mating displays: a peacock's tale. *Anim. Behav.* **102**, 241–250.
Garcia, M., Charrier, I. and Iwaniuk, A. N. (2012). Directionality of the drumming display of the ruffed grouse. *The Condor* **114**, 500–506.
Gerhardt, H. C. (1992). Conducting Playback Experiments and Interpreting their Results. In *Playback and Studies of Animal Communication*, pp. 59–77. Boston, MA: Springer.
Greenfield, M. D. (2002). *Signalers and Receivers: Mechanisms and Evolution of Arthropod Communication*. New York, USA: Oxford University Press.
Hagelin, J. C. (2002). The kinds of traits involved in male—male competition: a comparison of plumage, behavior, and body size in quail. *Behav. Ecol.* **13**, 32–41.
Hart, N. S. (2002). Vision in the peafowl (Aves: *Pavo cristatus*). *J. Exp. Biol.* **205**, 3925–3935.
Hartmann, M. J., Johnson, N. J., Towal, R. B. and Assad, C. (2003). Mechanical characteristics of rat vibrissae: resonant frequencies and damping in isolated whiskers and in the awake behaving animal. *J. Neurosci.* **23**, 6510–6519.
Heffner, H. E., Koay, G., Hill, E. M. and Heffner, R. S. (2013). Conditioned suppression/avoidance as a procedure for testing hearing in birds: The domestic pigeon (*Columba livia*). *Behav. Res. Methods* **45**, 383–392.
Heffner, H. E., Koay, G. and Heffner, R. S. (2016). Budgerigars (*Melopsittacus undulatus*) do not hear infrasound: the audiogram from 8 Hz to 10 kHz. *J. Comp. Physiol. A* **202**, 853–857.

Heidelbach, J. and Dambach, M. (1997). Wing-flick signals in the courtship of the African cave cricket, *Phaeophilacris spectrum*. *Ethology* **103**, 827–843.
Heinzel, H.-G. and Dambach, M. (1987). Travelling air vortex rings as potential communication signals in a cricket. *J. Comp. Physiol. A* **160**, 79–88.
Hill, E. M. (2017). Audiogram of the mallard duck (*Anas platyrhynchos*) from 16 Hz to 9 kHz. *J. Comp. Physiol. A* 1–6.
Hill, E. M., Koay, G., Heffner, R. S. and Heffner, H. E. (2014). Audiogram of the chicken (*Gallus gallus domesticus*) from 2 Hz to 9 kHz. *J. Comp. Physiol. A* **200**, 863–870.
Hillgarth, N. (1984). Social organization of wild peafowl in India. *World Pheas. Assoc. J.* **9**, 47–56.
Hingee, M. and Magrath, R. D. (2009). Flights of fear: a mechanical wing whistle sounds the alarm in a flocking bird. *Proc. R. Soc. Lond. B Biol. Sci.* rspb20091110.
Hörster, W. (1990). Vibrational sensitivity of the wing of the pigeon (*Columba livia*) — a study using heart rate conditioning. *J. Comp. Physiol. A* **167**, 545–549.
Imber, M. J. (1971). Filoplumes of petrels and shearwaters. *N. Z. J. Mar. Freshw. Res.* **5**, 396–403.
James, P. C. (1986). The filoplumes of the Manx Shearwater *Puffinus puffinus*. *Bird Study* **33**, 117–120.
Jones, I. L. and Montgomerie, R. (1992). Least auklet ornaments: do they function as quality indicators? *Behav. Ecol. Sociobiol.* **30**, 43–52.
Kalmijn, A. J. (1988). Hydrodynamic and Acoustic Field Detection. In *Sensory Biology of Aquatic Animals*, pp. 83–130. New York, USA: Springer.
Kämper, G. and Dambach, M. (1981). Response of the cercus-to-giant interneuron system in crickets to species-specific song. *J. Comp. Physiol.* **141**, 311–317.
Larsen, O. N. and Wahlberg, N. (2017). Sound and Sound Sources. In *Comparative Bioacoustics: An Overview* (ed. Brown, C.) and Riede, T.), pp. 3–61. Sharjah, UAE: Bentham Science Publishers.
Li, Q., Gao, K.-Q., Vinther, J., Shawkey, M. D., Clarke, J. A., D'Alba, L., Meng, Q., Briggs, D. E. G. and Prum, R. O. (2010). Plumage color patterns of an extinct dinosaur. *Science* **327**, 1369–1372.
Lieser, M., Berthold, P. and Manley, G. A. (2005). Infrasound in the capercaillie (*Tetrao urogallus*). *J. Ornithol.* **146**, 395–398.
Lieser, M., Berthold, P. and Manley, G. A. (2006). Infrasound in the flutter jumps of the capercaillie (*Tetrao urogallus*): apparently a physical by-product. *J. Ornithol.* **147**, 507–509.
Lindow, B. E. K. and Dyke, G. J. (2006). Bird evolution in the Eocene: climate change in Europe and a Danish fossil fauna. *Biol. Rev.* **81**, 483–499.
Löfvenberg, J. and Johansson, R. S. (1984). Regional differences and interindividual variability in sensitivity to vibration in the glabrous skin of the human hand. *Brain Res.* **301**, 65–72.
Lucas, A. M. and Stettenheim, P. R. (1972). Structure of Feathers. In *Avian Anatomy: Integument*, pp. 341–419. Washington, DC: US Department of Agriculture.
Lunichkin, A. M., Zhemchuzhnikov, M. K. and Knyazev, A. N. (2016). Basic elements of behavior of the cricket *Phaeophilacris bredoides Kaltenbach* (Orthoptera, Gryllidae). *Entomol. Rev.* **96**, 537–544.
Mack, A. L., Jones, J. and Nelson, D. A. (2003). Low-frequency vocalizations by cassowaries (casuarius spp.). *The Auk* **120**, 1062–1068.

Markl, H. (1983). Vibrational Communication. In *Neuroethology and Behavioral Physiology*, pp. 332–353. Berlin: Springer.
Murray, T. G., Zeil, J. and Magrath, R. D. (2017). Sounds of modified flight feathers reliably signal danger in a pigeon. *Curr. Biol.* **27**, 3520–3525.e4.
Nakagawa, S. and Schielzeth, H. (2010). Repeatability for Gaussian and non-Gaussian data: a practical guide for biologists. *Biol. Rev.* **85**, 935–956.
Nakagawa, S. and Schielzeth, H. (2013). A general and simple method for obtaining R2 from generalized linear mixed-effects models. *Methods Ecol. Evol.* **4**, 133–142.
Necker, R. (1985a). Receptors in the skin of the wing of pigeons and their possible role in bird flight. In *Biona Report* (ed. Nachtigall, W.), pp. 433–444. Stuttgart, New York: Fischer.
Necker, R. (1985b). Observations on the function of a slowly-adapting mechanoreceptor associated with filoplumes in the feathered skin of pigeons. *J. Comp. Physiol. A* **156**, 391–394.
O'Neil, N. P., Charrier, I. and Iwaniuk, A. N. (2018). Behavioural responses of male ruffed grouse (*Bonasa umbellus, L.*) to playbacks of drumming displays. *Ethology* **124**, 161–169.
Ota, N., Gahr, M. and Soma, M. (2015). Tap dancing birds: the multimodal mutual courtship display of males and females in a socially monogamous songbird. *Sci. Rep.* **5**,.
Persons, W. S. and Currie, P. J. (2015). Bristles before down: A new perspective on the functional origin of feathers. *Evolution* **69**, 857–862.
Pinheiro, J., Bates, D., DebRoy, S. and Sarkar, D. (2017). *nlme 3.1-131: linear and nonlinear mixed effects models*.
R Core Team (2017). *R 3.3.3: A Language and Environment for Statistical Computing*. Vienna, Austria: R Foundation for Statistical Computing.
Rogers, P. H. and Cox, M. (1988). Underwater Sound as a Biological Stimulus. In *Sensory Biology of Aquatic Animals*, pp. 131–149. Springer, New York, NY.
Russell, R. A. (2011). Air vortex ring communication between mobile robots. *Robot. Auton. Syst.* **59**, 65–73.
Santer, R. D. and Hebets, E. A. (2008). Agonistic signals received by an arthropod filiform hair allude to the prevalence of near-field sound communication. *Proc. R. Soc. Lond. B Biol. Sci.* **275**, 363–368.
Saxod, R. (1978). Development of Cutaneous Sensory Receptors Birds. In *Development of Sensory Systems*, pp. 337–417. Berlin: Springer.
Seneviratne, S. S. and Jones, I. L. (2008). Mechanosensory function for facial ornamentation in the whiskered auklet, a crevice-dwelling seabird. *Behav. Ecol.* **19**, 784–790.
Seneviratne, S. S. and Jones, I. L. (2010). Origin and maintenance of mechanosensory feather ornaments. *Anim. Behav.* **79**, 637–644.
Shen, J.-X. (1983). A behavioral study of vibrational sensitivity in the pigeon (*Columba livia*). *J. Comp. Physiol.* **152**, 251–255.
Shimozawa, T., Murakami, J. and Kumagai, T. (2003). Cricket Wind Receptors: Thermal Noise for the Highest Sensitivity Known. In *Sensors and Sensing in Biology and Engineering*, pp. 145–157. Berlin: Springer.
Sisneros, J. A. (2015). *Fish Hearing and Bioacoustics: An Anthology in Honor of Arthur N. Popper and Richard R. Fay*. Berlin: Springer.
Smith, W. F. (2010). *Waves and Oscillations: A Prelude to Quantum Mechanics*. New York, USA: Oxford University Press.
Sofroniew, N. J. and Svoboda, K. (2015). Whisking. *Curr. Biol.* **25**, R137–R140.
Steinmann, T. and Casas, J. (2017). The morphological heterogeneity of cricket flow-sensing

hairs conveys the complex flow signature of predator attacks. *J. R. Soc. Interface* **14**, 20170324.
Stettenheim, P. R. (2000). The integumentary morphology of modern birds—an overview. *Am. Zool.* **40**, 461–477.
Taylor, A. M., Bonser, R. H. C. and Farrent, J. W. (2004). The influence of hydration on the tensile and compressive properties of avian keratinous tissues. *J. Mater. Sci.* **39**, 939–942.
Toole, F. E. (2008). *Sound Reproduction: Loudspeakers and Rooms*. Oxford, UK: Focal Press.
Weir, K. A. and Lunam, C. A. (2011). The Structure and Sensory Innervation of the Integument of Ratites. In *The Welfare of Farmed Ratites*, pp. 131–145. Berlin: Springer.
Weiss, I. M. and Kirchner, H. O. K. (2010). The peacock's train (*Pavo cristatus* and *Pavo cristatus mut. alba*) I. structure, mechanics, and chemistry of the tail feather coverts. *J. Exp. Zool. Part Ecol. Genet. Physiol.* **313A**, 690–703.
Williams, C. L., Hagelin, J. C. and Kooyman, G. L. (2015). Hidden keys to survival: the type, density, pattern and functional role of emperor penguin body feathers. *Proc R Soc B* **282**, 20152033.
Yorzinski, J. L., Patricelli, G. L., Babcock, J. S., Pearson, J. M. and Platt, M. L. (2013). Through their eyes: selective attention in peahens during courtship. *J. Exp. Biol.* **216**, 3035–3046.

Figure 1

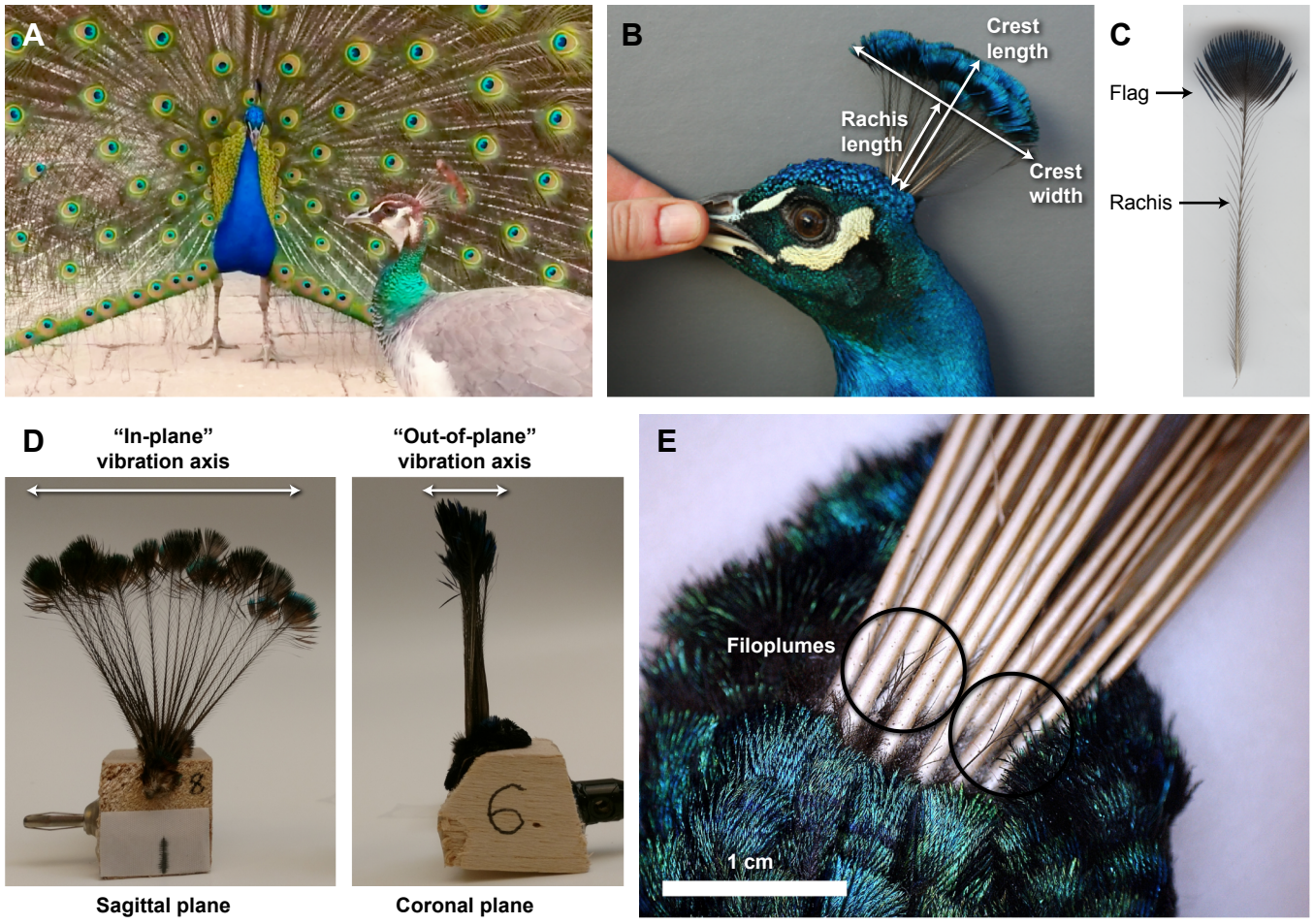

Figure 2

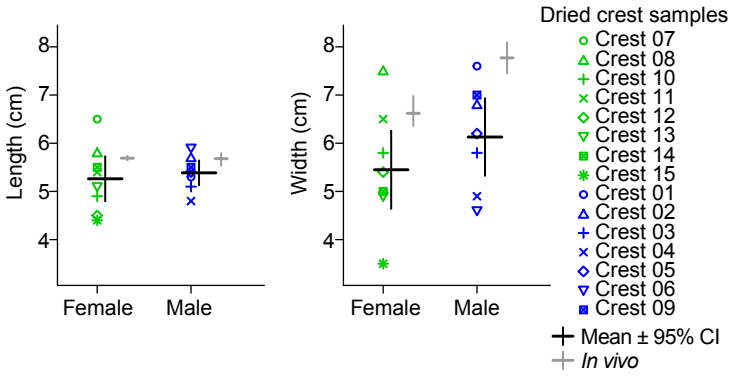

Figure 3

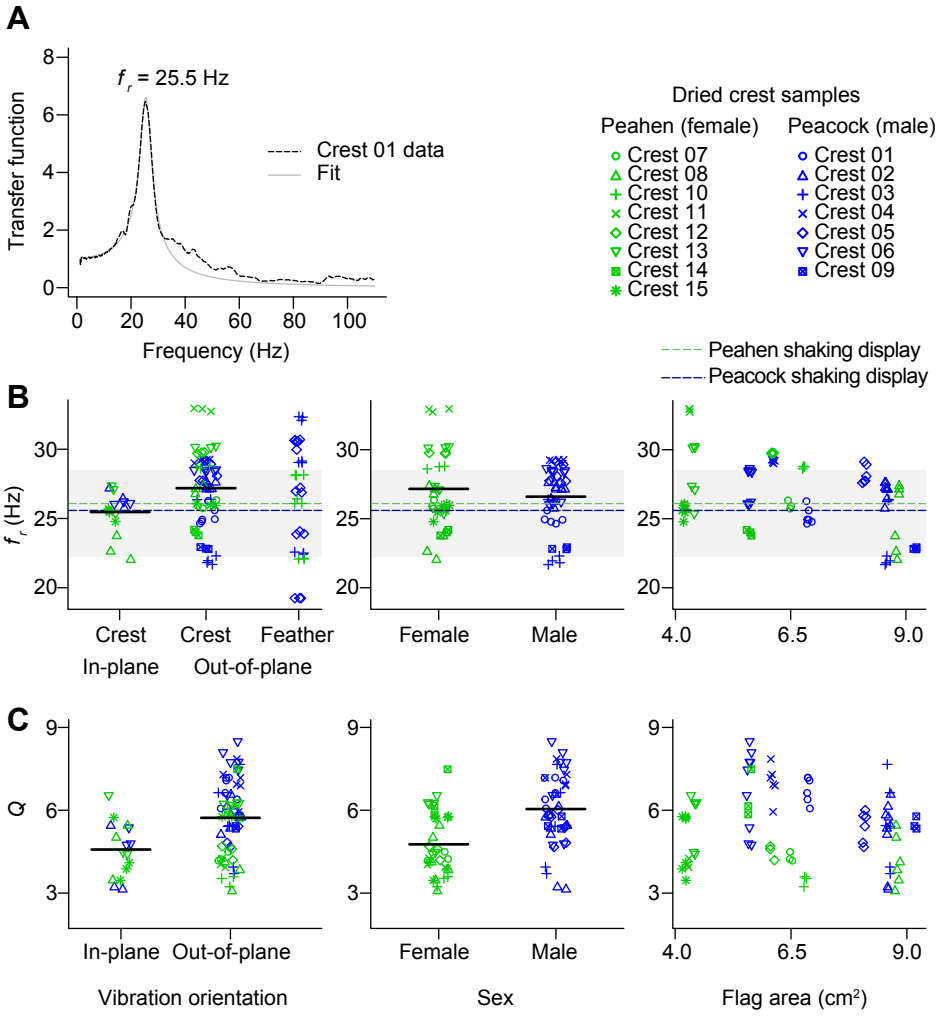

Figure 4

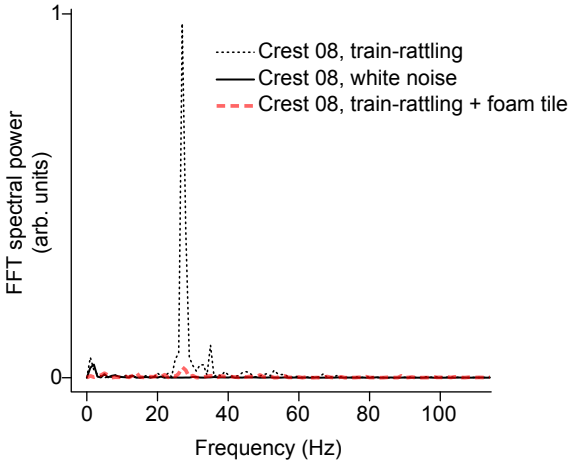

Figure 5

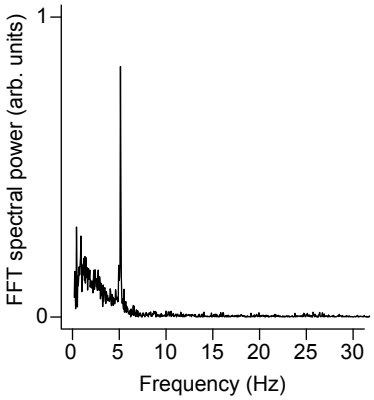

Figure 6